Chapter 6

Organic Thin-Film Transistor: Basics, Process Development and Electrical Characteristics

Today's microelectronics is based on the use of highly pure and high performance semiconductors like mono-crystalline Si, GaAs, InP, etc. These materials can provide carrier mobility in the order of 10^3 cm^2/Vs at room temperature, offer long carrier lifetime, can be precisely doped and patterned with accuracy better than 100 nm. In this way, they profit at best of the device speed and manufacture complex systems on chip that are capable to receive, memorize, elaborate and transmit enormous quantity of information, making possible like PCs, mobile phones and almost every commercial electronic products around our daily life [6.1].

Not all electronics, however, requires high performance. Some devices simply have to cover large areas, e.g. AMLCD, or must be manufactured with extremely low cost and disposable. Other devices have to be integrated with personal stuff or on a plastic substrate such as smart cards, car keys or identification tags. For this kind of applications, large area coverage, mechanical robustness and cheap manufacturing are much more important than the intrinsic performance, and that's why organic semiconductors draw so much attention recently. Moreover, device performance of organic thin film transistors (OTFTs) now rivals or exceeds that of amorphous silicon devices; the low process temperature of OTFTs allow fabrication on a range of surfaces including cloth, paper and polymeric substrates [6.2], [6.56], [6.57]. Nowadays the OTFTs have been successfully applied to AMOLED/AMLCD panels, photovoltaic cells, photodetectors, analog/digital circuits, gas sensors, etc. [6.3] – [6.8].

In this chapter, we will start with a briefly discussion of background information of

OTFTs like types of organic materials, the deposition method, specific patterning technique, basic electrical properties and current issues about OTFTs, etc. Then we chose one of the most popular organic materials, poly-3-hexylthiophene (P3HT), and designed a series experiments to optimize the spin-on deposition conditions, OTFT structures as well as electrical characteristics.

6.1 Basics of OTFTs

6.1.1 Classification of Organic Materials

Polymers and organics in general, have been traditionally employed only as insulating materials until 1977, when the first report on an electrically conduction polymer appeared [6.9]. A few years later, the first polymer-based transistor was fabricated in 1983 [6.10]. Today, all semiconductors used in organic TFTs are *conjugated* organic materials. In this class of materials single and double carbon bonds alternate along the molecule backbone. According to the molecular weight of materials, the organic semiconductors can be roughly divided into two types: oligomers and polymers [6.1], [6.11].

Oligothiophenes – The chemical scheme of oligothiophenes (nT, where n stands for the number of thiophene units) is shown in Fig. 6-1(a). This was the first report of an OTFT made with a small conjugated molecule [6.12]. Oligothiophenes, 4T – 8T, are either non-substituted or substituted at both ends by a linear alkyl group, possessing hole mobility from 10^{-3} to 10^{-2} cm^2/Vs.

Pentacene – As a member of oligomers, pentacene consists of five aligned condensed benzene rings as shown in Fig. 6-1(b), which was extensively studied during 1960s and 1970s. Due to its highly ordered morphology close to that of a single crystal, mobility up to 2 cm^2/Vs and high ON/OFF current ratio reaching 10^8 were reported under a delicate vacuum deposition process [6.13], [6.14]; thus pentacene has became the most promising candidate

for OTFTs in AMLCD/AMOED industry.

Polymers – Most widely investigated polymer-type semiconductor today is poly-3-hexylthiophene (P3HT), which consists of a thiophene ring and a hexyl side chain as shown in Fig. 6-1(c). Owing to the characteristics of the alkyl-group side chain, this type of organic material is solution-processed. The performance of polymers stands roughly one order of magnitude below that of the small molecules for the fact of a poorer ordering. Detailed characteristics of P3HT will be described later in this chapter.

N-type semiconductors – Most of the organic semiconductors investigated so far are p-type in their non-intentionally doped form. There are several reasons why only a limited number of high-performance n-channel semiconductors have been discovered so far. First, most organic materials tend to transport holes better than electrons and thus there are less organic n-channel materials available. Second, the performance of n-channel semiconductors is easily degraded after exposure to air since oxygen can act as a trap to oxidize some negative charge carriers [6.15]. This can be explained by C_{60}, the mobility of which can be as high as 0.08 cm^2/Vs in ultra high vacuum but falls by 4 or 5 orders of magnitude upon exposure to air [6.16]. Nevertheless, materials with better stability in air and high electron mobility of 0.03 cm^2/Vs has been developed such as $F_{16}CuPc$ (Pc = phthalocyanine), as shown in Fig. 6-1(d) [6.17].

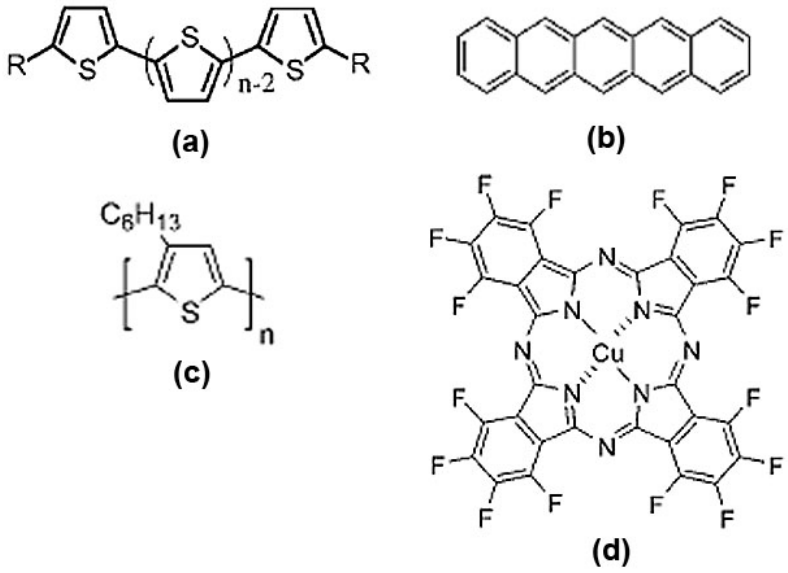

Figure 6-1 Chemical structure of (a) unsubstituted (R = H) and alkyl end-substituted (R = C_nH_{2n+1}) oligothiophenes (b) Pentacene, (c) poly-3-hexylthiophene, and (d) n-channel Copper Hexadeca – fluoro – phthalocyanine, $F_{16}CuPc$

6.1.2 Deposition Process of Organic Semiconductor

Electropolymerization – This technique is for the synthesis of conducting polymers. However, since electropolymerization only occurs on conducting substrates, this method cannot deposit polymers directly on the insulating layer. Besides, the deposited polymer has to be reduced (generally electrochemically) from its oxidized/conducting form to become semiconducting, so that this technique is no longer used in the fabrication of OTFTs today [6.11].

Vacuum evaporation – Oligomers such as pentacene is generally deposited through vacuum evaporation. The organic material is put into an ultra high vacuum chamber and then evaporated via Joule heat or electron beam. If proper controlling the deposition rate and the substrate temperature during evaporation process, highly ordered films with satisfactory field-effect mobility can be obtained. Moreover, pentacene can also be evaporated from a crucible cell with a nozzle, namely energetic cluster evaporation (ECE), to reduce the interface states at the interface of gate insulator [6.58]. Primary drawback of vacuum

deposition is probably the sophisticated instrument and high production costs.

Langmuir-Blodgett Technique – an alternative means to make well-organized thin films of small molecules. However, this technique is in principle restricted to amphiphilic molecules, composed of a hydrophobic chain and a hydrophobic head group, basically not the case for most active layer materials used in OTFT fabrication. Nevertheless, a similar "layer-by-layer" nanoassembly method was developed to deposit the gate insulating layer of OTFTs with precise thickness control [6.18].

Solution-processed deposition – The key feature that makes organic semiconductors attractive for low-cost manufacturing is the possibility for them to be deposited from spin coating, enabling very homogeneous films with perfect control of their thickness over a large area. Moreover, only solution-processed organic semiconductors and organic conducting electrodes can be deposited by ink-jet printing, micro-contact printing by rubber stamp or screen printing methods, contributing to a full integration with OLED devices on plastic substrates by reel-to-reel process (also called roll-to-roll process) with low production costs [6.19]-[6.22]. Major disadvantage of solution-processed deposition is that the selected solvent needs to be environmentally friendly. Most of the conjugated polymers are more soluble in chlorinated solvents such as chloroform and chlorobenzene, which are unacceptable for manufacturing. However, it's a pity that best mobility reported for P3HT was obtained with chloroform as the solvent. More efforts should be devoted to the research about using more environmentally friendly solvents such as xylene.

6.1.3 Conduction Mechanism

For conjugated organic materials, single and double carbon bonds alternate along the molecule backbone, which means all the p_z orbitals of the carbon atoms participating to either a double or a single bond from a sort of continuous π bond that is delocalized along the whole molecule. The hybridization of the p_z orbitals gives rise to splitting of their energy levels and

forms a sort of highest occupied molecular orbit (HOMO) analogous to the valence band of a conventional inorganic semiconductor. On the other hand, the anti-bonding π^* orbitals, with their higher energy, constitute the lowest unoccupied molecular orbit (LUMO) like the conduction band of inorganic semiconductor. Figure 6-2 illustrates this concept with an energy band diagram. Through the delocalized π and π^* orbitals, charge transport within one molecule is relatively easy.

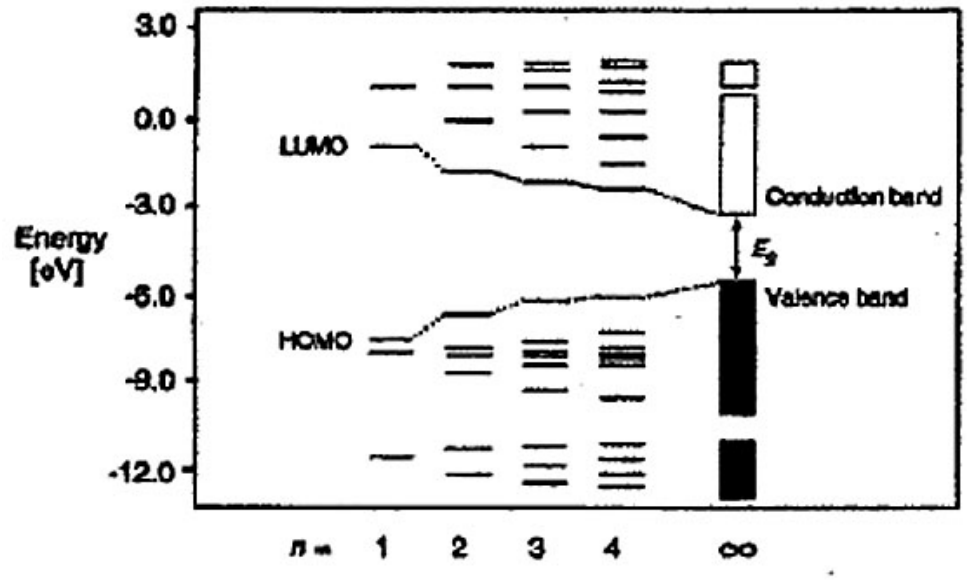

Figure 6-2 The energy levels of oligo and poly-thiophenes as a function of the number of conjugated units

In contrast, transport from one molecular to another is much more difficult due to a small energetic coupling between molecules held by weak van der Waals forces of ~10 kcal/mol [6.23]. Generally, intermolecular transport cannot be described with the conventional band theory, but as carrier hopping between molecular localized states, which is phonon assisted. Accordingly, unlike the case of phonon scattering for conventional semiconductor, the mobility increases with temperature following a law of the form $\mu = \mu_0 \exp[-(T_0/T)^{1/\alpha}]$, where α is an integer ranging from 1 to 4. However, for highly ordered organic material, the explanation for inter-molecular conduction by hoping process may face

some controversy [6.11].

Another characteristic of organic material is that most polymers conduct one kind of carrier only, either electron or hole. Because of the nature of large band gap (e.g. E_g of P3HT = 2.2 eV), the active layer cannot be inversed by thermal energy at room temperature (i.e. slow generation rate of inversion layer). Therefore, OTFTs operate in the accumulation mode at its ON state and depletion mode at its OFF state.

In summary, the classification, deposition method, field-effect mobility and conducting carrier type of several commonly used semiconductors are listed in Table 6-1.

Table 6-1 Characteristics of some of the most commonly used semiconductors

	Material	Film Deposition Method	Carrier Mobility	Carrier type
	c-Si	Epitaxial	1500/480	e^-/h^+
	a-Si:H	PECVD	0.1-1/<0.1	e^-/h^+
Oligomers	Pentacene	1. Monocrystalline growth 2. vacuum evaporation 3. solution-processed from precursor	1.7/2.7 1.2 10^{-2}	e^-/h^+ h^+ h^+
	α-sexithiophene	Vacuum evaporation	0.7/1.1	e^-/h^+
	Perylene	Monocrystalline growth	5.5	e^-
	C_{60}	Vacuum evaporation	0.002-0.08	e^-
	TCNQ	Vacuum evaporation	1.9×10^{-5}	e^-
	$F_{16}CuPc$	Vacuum evaporation	0.03	e^-
Polymers	Regioregular-P3HT	Solution processed	0.01-0.1	h^+
	Polyfluorene copolymers	Solution processed	0.03	h^+
	PTV	Solution processed from precursor	10^{-3}	h^+

6.1.4 Other Specific Material or Circuit Considerations

Thermal conductivity – In case of silicon ICs, the difference in junction and ambient temperature can be as high as 125°C – 1150°C. For the case of densely packed organic

semiconductors, the chip will burn out as soon as it is turned ON [6.24], [6.25]. However, compared to silicon, the thermal conductivity of a typical organic material (6.9×10^{-3} $Wcm^{-1}K^{-1}$) is about three orders of magnitude lower. Consequently, how speeding up heat dissipation as well as examining the stability issues associated with self-heating phenomenon require special considerations.

CMOS circuits – Inorganic semiconductor such as Si or GaAs can be easily doped as p-type or n-type through proper impurities, but few organic materials, especially polymeric type, can conduct holes and electrons simultaneously. The fabrication of integrated complementary OTFTs is thus required two different organic semiconductors, which may add some process complexity. Besides, the difference of carrier mobility between n-type and p-type semiconductors is very large, for example, μ_e of $F_{16}CuPc$ = 0.03 and μ_h of pentacene = 1 cm^2/Vs from Table 6-1. For an ideal complementary circuit, this means $(W/L)_n/(W/L)_p$ = 33.3, which is not desirable in a view point of circuit design.

Operation voltage – It is well known that the threshold voltage of a transistor is affected by the fix oxide charges, interface states and trap states in the bulk of active area [6.26]. For OTFTs, the interface and trap states in the organic active layer are very high, so that the general operation voltage ranges around 30 V or larger, which does not coincide with the trend of low power design for mobile electronics. Reducing the thickness or increasing the dielectric constant of the gate insulating layer thus becomes important research topics.

Reliability considerations – More and more investigations reported that the electrical characteristics of OTFTs degraded significantly when exposed to the air, O_2 or moisture environments [6.26], [6.27]. Also the n-channel OTFTs are more sensitive to atmosphere and water due to the instability of the organic anions [6.28]. Accordingly, the environment control of fabrication process of OTFTs and a proper capping layer after production is required to protect the organic materials from being damaged. Besides, hot carrier or self-heating effect induced instability problems commonly observed in inorganic a-Si or poly-Si TFTs are not

well understood for the case of OTFTs. We will investigate the reliability issues of OTFTs in *chapter 7*.

6.2 Introduction to Poly-3-hexylthiophene, P3HT

Soluble organic semiconductors have recently attracted particular interest, since these materials can be easily spun-coated to from circuits for disposable electronics on a plastic substrate. One of the first solution-processable organic semiconductors used in OTFTs was poly-3-hexylthiophene or P3HT, in which the addition of alkyl side-chains enhances the solubility of the polymer chains [6.29]. However, the morphology of P3HT can be very different depending on the deposition methods, purity of P3HT and solvents. We'll briefly discuss these topics before starting the experimental design.

6.2.1 The Molecular Structure of P3HT

The structure of the polymer chain of P3HT had been shown in Fig. 6-1(c) and is redrawn with more details here in Fig. 6-3. The 3-alkyl substituents can be incorporated into a polymer chain with two different regioregularities: head to tail (HT) and head to head (HH) [6.30]. Here R represents the alkyl side chain (C_6H_{13} for P3HT), which allows P3HT to be dissolved in solvents like chloroform.

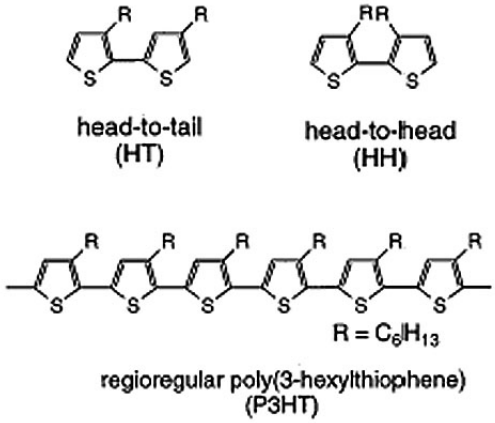

Figure 6-3 Molecular structure of poly-3-hexylthiophene

A regiorandom P3HT consists of both HH and HT 3-hexylthiophenes in a random pattern while a regioregular P3HT has only one kind of 3-hexylthiophene backbone, either HH or HT. With a higher ordering, or regioregularity, much higher field-effect mobility can be obtained than those polymers with regiorandom (disordered side chains) structure [6.31]. More interestingly, polymers with regioregular molecular structure exhibit very different properties from their regiorandom counterpart including a smaller band gap, better ordering and crystallinity in solid states and substantially improved electroconductivities [6.32]. The P3HT material we used in this work consists 98% or more head-to-tail linkages. Except regioregularity, the length of alkyl side chain also affects the ordering and hence the mobility. A study of P3ATs (A=hexyl, octyl, dodecyl, hexadecy) showed that the mobility decreases with increasing the length of side chain [6.33].

6.2.2 Solvents and Purification Process for P3HT

P3HT has the highest solubility in chloroform, and its solubility in various solvents is in the following order: chloroform > xylene > tetrahydrofuran (THF) > hexane > acetone > methanol [6.34]. The field effect mobility of 0.1 cm^2/Vs is achieved by chloroform as the solvent while the mobility is only 6×10^{-4} by tetrahydrofuran. By using large solubility difference between xylene and methanol, the P3HT molecules can be “reprecipitated” to reduce the concentration of impurities. The extracted samples can be further purified through chloroform/methanol solvents for a long reprecipitation period [6.35]. Besides, It is reported that P3HT prepared at very low temperature (-40^oC) with $FeCl_3$ as a catalyst can improve the crystallinity and regularity of the polymer. The incorporated dopants (such as oxygen) during synthesis process can also be dedoped in a 30% ammonia-ethanol solution for 1 hr [6.36] or by adding a few drops of hydrazine (N_2H_4) [6.37].

6.2.3 Deposition Method and Surface Morphology

Two different methods are usually applied to deposit the P3HT film. One is spin coating while the other is dip coating (or solution casting), in which the samples are dipped in the P3HT solution and we wait until the solvents evaporates naturally. The mobility of spin-coated films is usually lower than that of the cast films, perhaps because for cast films, the evaporation rate of solvents is slower and results in a slower crystal growth with better ordered polymer structure [6.32], [6.38].

After being deposited on the substrate, P3HT backbones may form two different morphologies, that is, edge-on or face-on of the lamella structure as shown in Fig. 6-4. The mobility is much higher for edge-on structure since the carriers can move more efficiently through intra-chain transport along the direction of π-π stacking [6.39]. Moreover, highly aligned film of regioregular P3HT is fabricated by friction transfer technique; the main chains of P3HT orient within 13 degree along the dragging direction contribute to higher mobility enhanced by a factor of 2 – 70 compared with the non-aligned spin-coated P3HT film [6.40], [6.41].

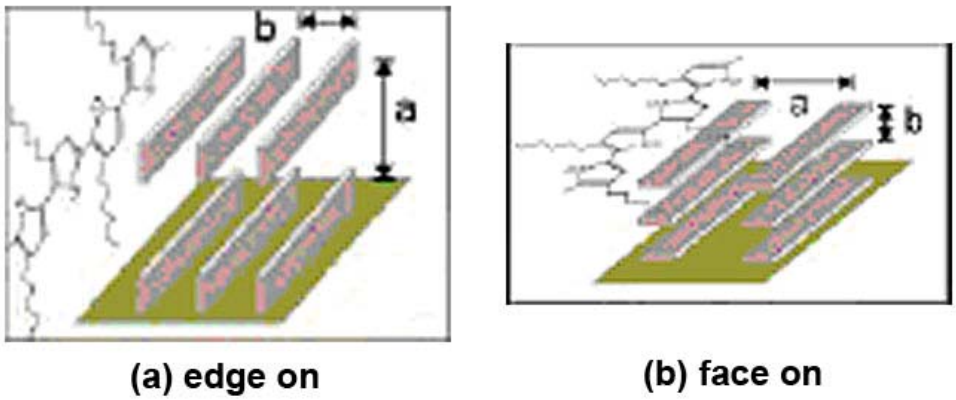

Figure 6-4 Two different orientations of ordered P3HT lamella structure with respect to the substrate

6.3 Optimization of Spin-on Conditions of P3HT

Since P3HT is generally solution-processed, the conditions of spin-coating including the solvents, the weight percentages of P3HT and the curing temperatures, etc. should be optimized to acquire satisfactory electrical properties of OTFTs. In this section, we utilized chloroform and xylene as the solvents of P3HT and performed a series experiments.

6.3.1 Experimental: Sample Preparation

The P3HT organic TFTs were fabricated on a heavily doped n^+ silicon substrate with thermally grown gate insulator and thick field oxide, as shown in Fig. 6-5(a). First, phosphorus atoms were diffused into an n-type Si wafer by $POCl_3$ to create a common gate electrode. A field SiO_2 layer with a thickness of 500 nm and a thin gate oxide layer with a thickness of 100 nm were subsequently grown in a furnace. Afterwards, source/drain regions were defined using photo lithography process followed by the thermal evaporation of a 20 nm-thick layer of Ti as an adhesion layer and a 100 nm-thick layer of Pt as a contact material. The wafer was then immersed in acetone to lift off the photo resist and form the source/drain regions. A comb geometry, as depicted in Fig. 6-5(b) for the source/drain contacts, is adopted to minimize the device area and the associated gate to source/drain leakage current. A typical channel width W was in the range of 100 ~ 10,000 μm and a channel length was 10 ~ 50 μm.

The samples, after S/D patterning, were treated with hexamethyldisilazane (HMDS) to improve adhesion and regioregularity between the polymer chain and the oxide surface. After treating SiO_2 surface with HMDS, the hydroxyl groups at the oxide surface would be replaced by methyl groups and the apolar nature of these groups apparently attract the hexyl side chains of P3HT, favoring lamellae with an edge-on orientation [6.39].

Next, P3HT of 0.1, 0.3, 0.8 or 2.0 wt. % dissolved in chloroform or xylene was filtered through a 0.2-μm pore-size PTFE filter and then spun onto the wafer surface, which was then

cured at 120℃. Here the atomic force microscope (AFM) was also utilized to observe the surface morphology of P3HT deposited with different weight percentage, spin speed and curing temperature. P3HT and its solvent were both purchased from Aldrich chemical company and no further purification or sublimation was performed.

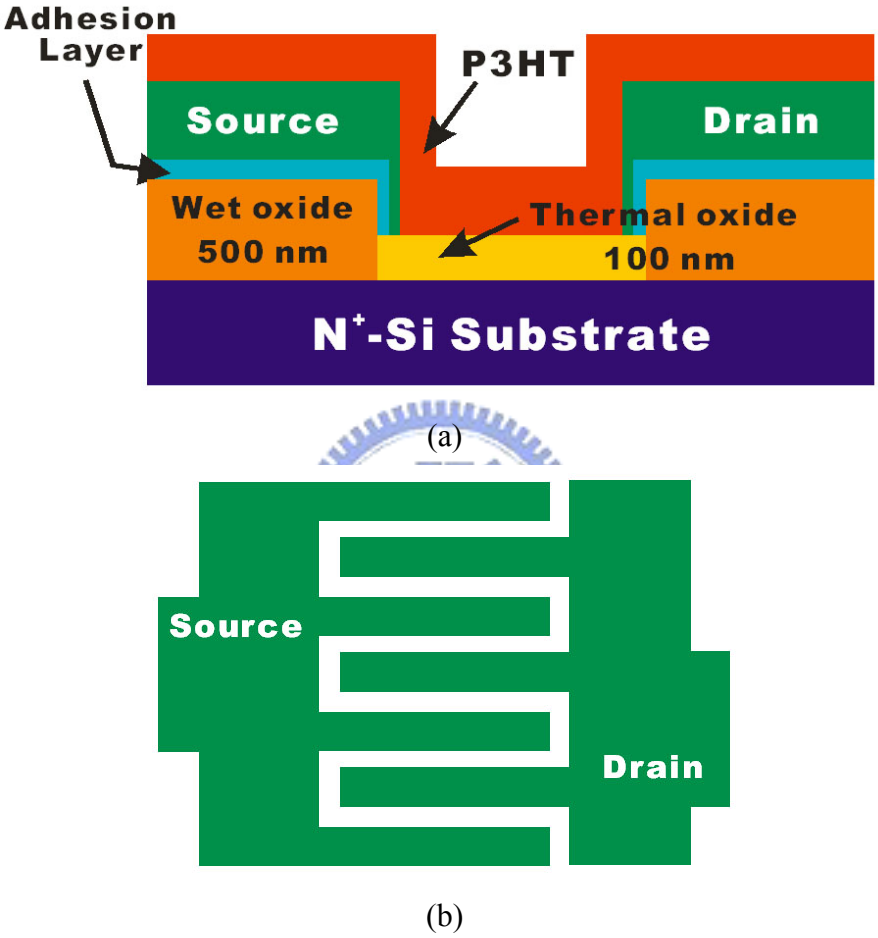

Figure 6-5 (a) Schematic diagram of OTFT with the field oxide layer on the source/drain region, and (b) comb structures for source/drain electrodes

The detailed process flow of OTFTs was listed below:

1. Initial RCA cleaning
2. Phosphorus diffusion for conductive common gate electrode: $POCl_3$ source, 800^{o}C by furnace; pre-deposition for 30 min followed by drive-in for another 1 hour
3. 500 nm field-oxide layer: furnace wet oxidation at 1050^{o}C

4. Mask #1: Active area definition
5. Wet etching of active area: buffered oxide etcher (NH_4F : HF = 6 : 1)
6. P.R. strip/RCA cleaning
7. 100 nm gate oxide: furnace dry oxidation at 1050^{o}C
8. Mask #2: Source/Drain electrodes definition
9. Ti/Pi = 20 nm/100 nm as the adhesion/electrode layer: Dual E-Gun evaporation system at base pressure = 2×10^{-6} torr; metals were deposited continuously without breaking vacuum
10. P. R. lift-off to form source/drain electrodes: in ACE with ultrasonic agitation
11. ACE + IPA cleaning
12. HMDS treatment: 150^{o}C, 10 torr
13. Spin-on P3HT: (typically) 0.3 wt. % P3HT in chloroform, 500 ~ 2000 rpm., curing temperature 120^{o}C

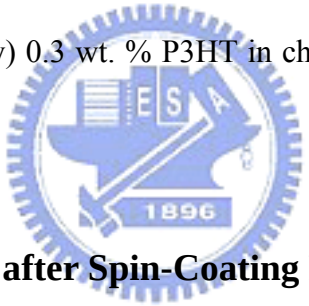

6.3.2 Physical Observation after Spin-Coating P3HT

Figure 6-6(a) exhibits the surface morphology of the deposited P3HT film for P3HT of 0.3 wt. % in xylene. Many clusters of undissolved P3HT powder, despite having been filtered, are still observed. For P3HT dissolved in chloroform, however, no micro particles of P3HT can be found as shown in the AFM photographs of Fig. 6-6(b) ~ 6-6(e) even the P3HT wt. % as high as 2.0. Besides, the rms value of surface roughness reaches 0.82 nm at 0.3 wt. % and then increases significantly at 0.8 and 2.0 wt. %. Pin holes are commonly observed in Fig. 6-6(e), which may attribute to the suddenly evaporation of solvents through a thick P3HT layer. No apparent grain/grain-boundary structure was found in the AFM photographs because the P3HT thin film is a long-chain polymer with a lamella layer structure.

Table 6-2 summarizes the surface roughness of the P3HT film (dissolved in xylene) with respect to spin speed and the post-annealing temperature. The surface roughness of the

P3HT film slightly declines as the spin speed increases, since a higher spin speed results in a better distribution of the solvent and, therefore, a smoother surface. For surface roughness of P3HT after post annealing, although the melting temperature of P3HT is 178℃, increasing the film to a moderately close temperature is expected to thermodynamically allow a change triggered by a conformation change within the alkyl-group. B. A. Mattis et al. found that the roughness was increased after a high-temperature annealing step, indicating that the P3HT film was rearranged into a more disorganized state [6.42]. Nevertheless, the post-annealing temperature (up to 170℃) negligibly affects the surface roughness, according to the experimental results presented herein. The authors speculated that the deposited P3HT film with xylene as a solvent is too thin to reflect the conformation change of P3HT polymers in the surface morphology.

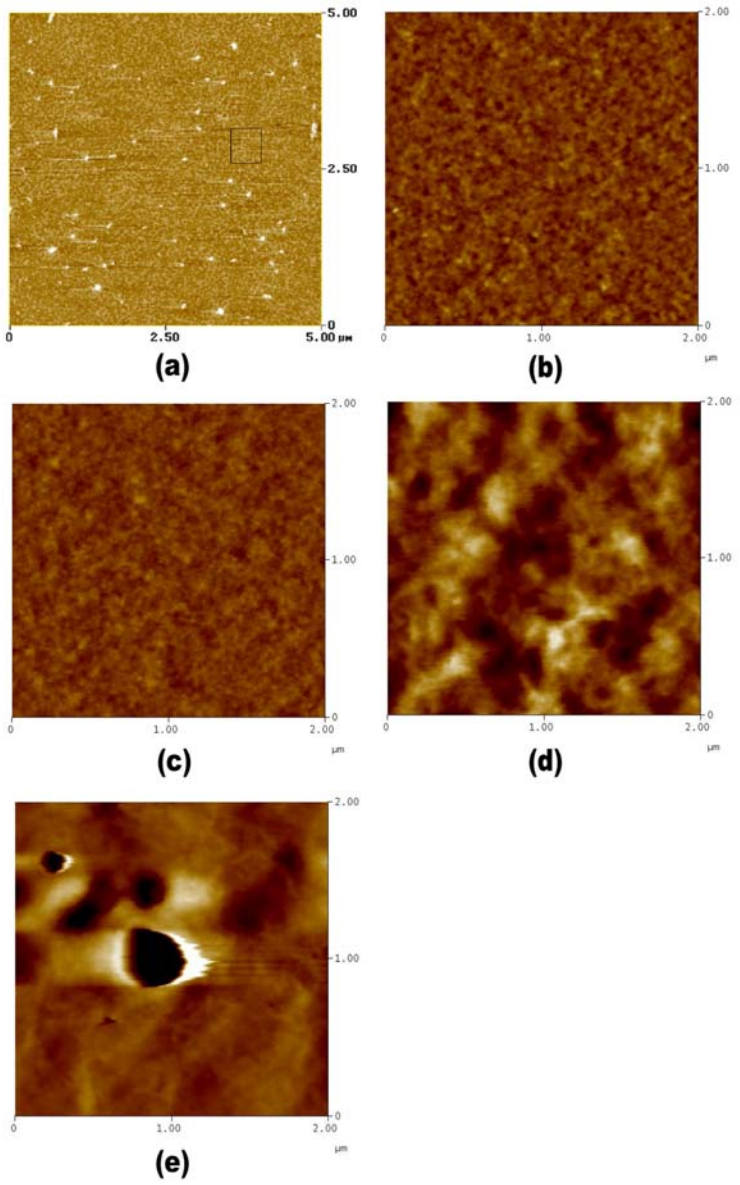

Figure 6-6 Surface morphology measured by atomic force microscope of the P3HT films deposited with different conditions: (a) 0.3 wt. % in xylene, (b) 0.1 wt. % in chloroform, (c) 0.3 wt. % in chloroform, (d) 0.8 wt. % in chloroform, and (e) 2.0 wt. % in chloroform

Table 6-2 Surface roughness of the P3HT film with respect to spin speed and the post-annealing temperature

Spin speed (rpm)	Annealing temperature (^{o}C)	Surface roughness of P3HT film (nm)
1000	170	0.45
2000	170	0.40
4000	170	0.39
6000	170	0.36
2000	R.T.	0.53
2000	100	0.32
2000	150	0.41
2000	170	0.36

At a spin-speed of 2000 rpm, the thickness of P3HT film deposited by xylene solution (0.3 wt. %) was 240 Å, which is much thinner than that deposited by chloroform (0.3 wt. %, 1140 Å). Both of them were estimated from the cross-sectional view obtained using the scanning electron microscope (SEM) as shown in Fig.6-7. Other optical methods such as ellipsometry or spectrometry, however, were not appropriate for measuring the thickness due to the non-regioregularity and the associated non-uniformity of the refractive index of P3HT.

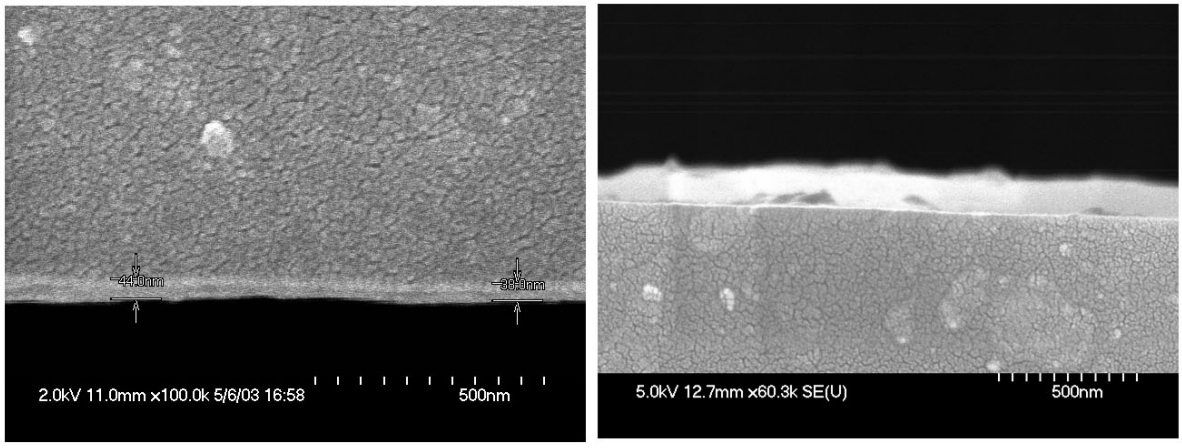

Figure 6-7 Thickness estimation of spin-on P3HT films by SEM cross-sectional view: (a) 0.3 wt.% in xylene, and (b) 0.3 wt.% in chloroform

6.3.3 Electrical Characteristics of OTFTs

Figure 6-8 compares the I_S - V_G and the mobility curves of OTFTs fabricated by different solvents. The field-effect mobility of OTFTs deposited by chloroform and xylene are 2.1×10^{-3} and 7.0×10^{-4} cm^2/Vs, respectively. Although the boiling point of xylene (140^oC) is higher than that of chloroform (41^oC), the slower evaporation rate of xylene does not relate to the crystallinity of P3HT and the mobility. Contrarily, based on the above observation that the thickness of P3HT prepared by xylene solution is only 240 Å, the resulted inferior mobility is due to the poor step coverage of P3HT film on the S/D electrodes, disordered lamella structure and strong surface scattering effect owing to the vertical gate electric field. Nevertheless, the gate controllability is enhanced for a thin active layer and thus the subthreshold swing of devices prepared by xylene solution becomes steeper than those prepared by chloroform. Since chloroform is toxic to the neural system and the usage is restricted or prohibited in some countries, xylene becomes an appropriate choice despite its low mobility and solubility to P3HT.

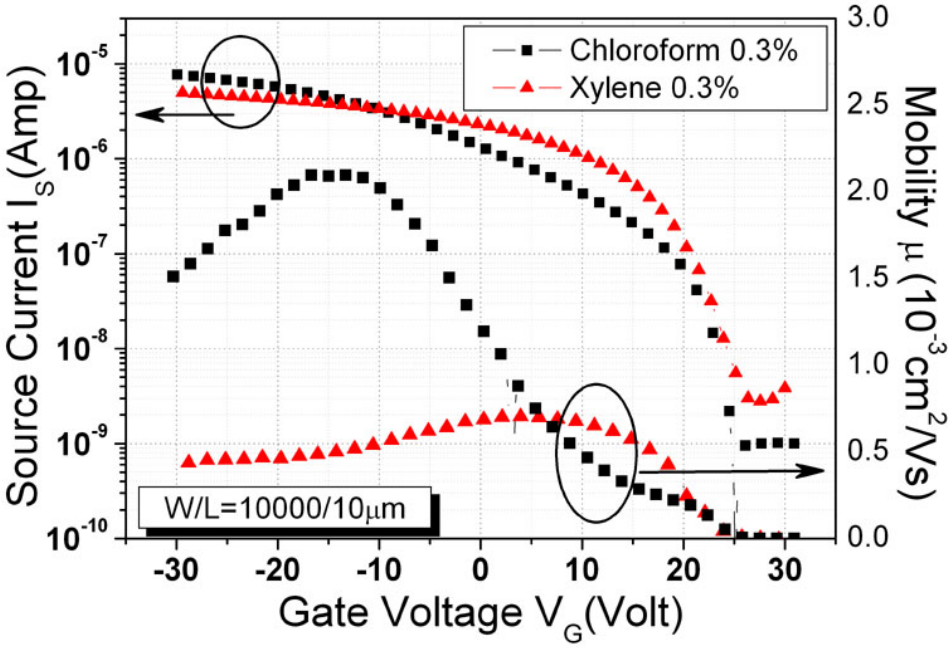

Figure 6-8 I_S - V_G and mobility curves of the OTFTs fabricated by xylene or chloroform solution

Figure 6-9(a) illustrates the I_S - V_G curves of OTFTs fabricated by different weight percentages of P3HT in chloroform. The OTFTs exhibit satisfactory ON/OFF ratio, subthreshold swing and leakage current for the concentration of P3HT below 0.3%. However, the ON/OFF current ratio of 0.8% and 2.0% samples reduced drastically to less than 10, primarily resulting from the increase of the leakage current. Figure 6-9(b) shows the I_S - V_D characteristics of OTFTs in their "OFF" state when a positive gate bias was applied. As the gate voltage increases, the channel would deplete while the off-current I_S gradually saturates, and thus I_S becomes independent of the drain voltage. Nevertheless, the I_S - V_D curves exhibits linear-like characteristics when the concentration of P3HT exceeds 0.8%. The total current in a polymeric TFT can be separated into two components – channel current (I_{ch}) and bulk current (I_{bk}) [6.43]. Assuming the bulk current can be represented as equation (6-1) according to Ohm's law:

$$I_{bulk} = \sigma \frac{W}{L} l \times V_{DS} \tag{6-1}$$

where σ is the carrier mobility and l is the thickness of the polymeric layer. Through the observed linear-like off-state leakage current, the conductivity of the P3HT film can be calculated as 2.92×10^{-5} S/cm by assuming l = 114 nm (as indicated in the SEM cross-sectional view). Suppose the μ_{FE} of P3HT film equals 2.5×10^{-3} cm^2/Vs, the corresponding dopant concentration is 7.3×10^{16} cm^{-3}, a larger value comparing to a typical 1×10^{16} cm^{-3} prepared by P3HT of 1 wt.% in chloroform [6.61].

To obtain an appropriate deposition concentration of P3HT, the dependence of the mobility and the ON/OFF current ratio versus various wt. % of P3HT in chloroform were plotted in Fig. 6-10. Different device geometries were examined and the values of mobility or ON/OFF ratio were averaged with at least five points, all of them exhibiting the similar trends. There is a maximum value for ON/OFF ratio as concentration of P3HT equals 0.3%. Additionally, we inferred that the largest field-effect mobility would also occur at 0.3%

because of the lowest value of surface roughness as shown in Fig. 6-6(c). Although the peak value of mobility located at 0.8% in Fig. 6-10, we speculated that the lower parasitic resistance for P3HT of 0.8% causes a slightly over estimation of mobility. Besides, A. N. Aleshin et al. examined the electrical properties with respect to the P3HT concentration between 0.033 to 0.168% at extremely high spin speed [6.44]. At 0.06 – 0.07 wt. %, the mobility is below 1×10^{-3} cm^2/Vs at room temperature but the ON/OFF ratio can exceed 10^5. Therefore, a trade-off should be made between mobility and off-state leakage current.

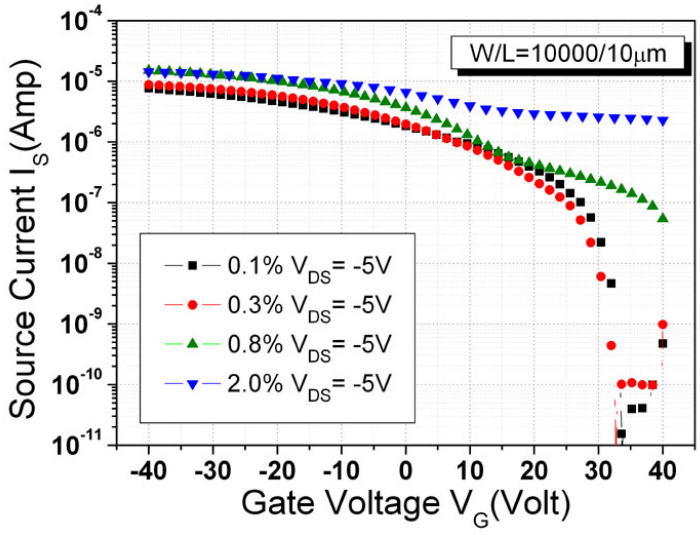

(a)

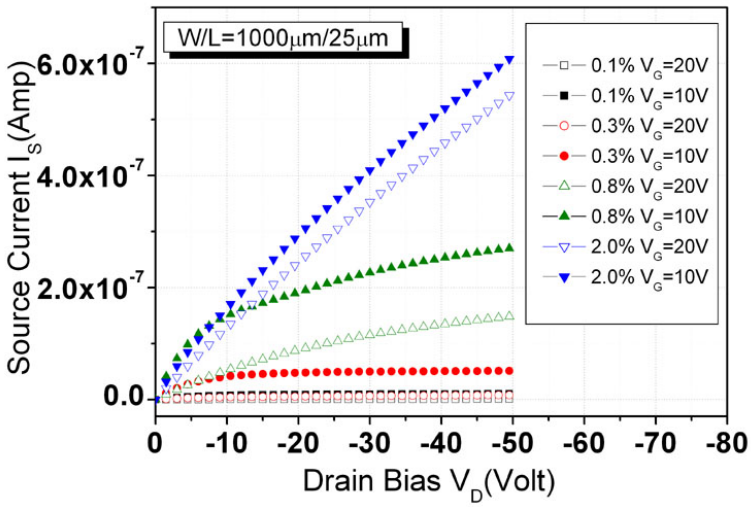

(b)

Figure 6-9 (a) I_S - V_G and (b) I_S - V_D curves of the OTFTs fabricated by different weight percentages of P3HT in chloroform

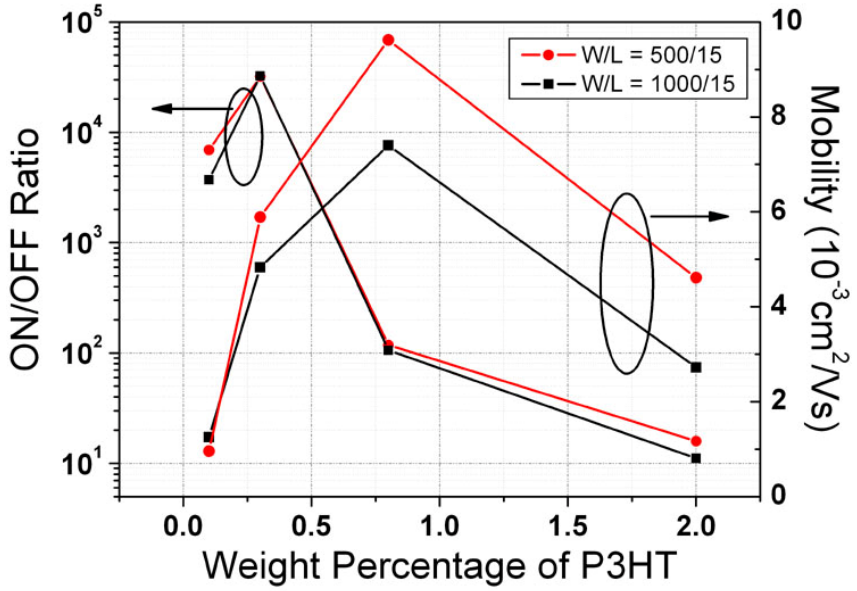

Figure 6-10 ON/OFF current ratio and mobility characteristics of OTFTs vs. various weight percentages of P3HT film

6.4 Structural Considerations of OTFTs

Similar to poly-Si TFTs with top gate and inverse staggered structures, OTFTs have two common architectures: top contact (TC) and bottom contact (BC), which represents the position of source/drain electrodes locating above or beneath the organic active layer. Besides, it is found that anomalous leakage current through the gate dielectric layers, especially those through high-k gate materials, would reduce the ON/OFF current ratio and increase power consumption [6.45]. In this section, we will examine the electrical characteristics of OTFTs with different architectures and propose an effective isolation structure by field oxidation to suppress the leakage current through the common thin gate oxide region.

6.4.1 Experimental: Sample Preparation

Top-contact structure – To construct the top-contact type device, we first fabricated the OTFTs by spin coating a P3HT film onto a highly doped n^+ Si wafer with a 100 nm thermal oxide layer. Here the P3HT solution was prepared by 0.3 wt. % P3HT in xylene

solvent. Platinum source/drain contacts were then deposited to the surface of the P3HT film immediately by Dual E-Gun evaporation system through a shadow mask (or namely metal mask). Typical channel width W is in a range of 100 ~ 5000 μm while typical channel length is in a range of 30 ~ 200 μm. The process flow for fabrication a top-contact type OTFT is depicted in Fig. 6-11

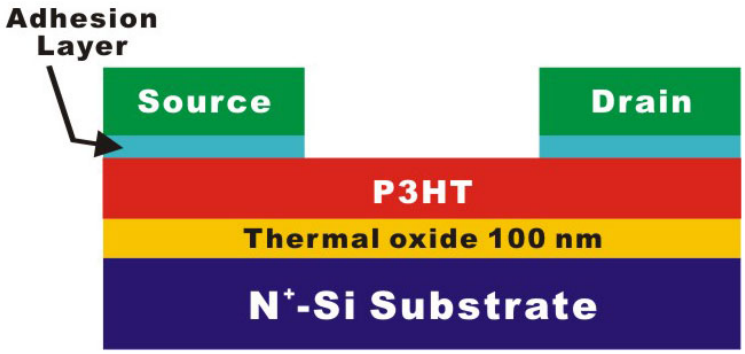

Figure 6-11 Process flow of a TC-OTFT

Bottom-contact structure – The process described in *Section 6.3.1* is basically a bottom contact configuration with thick field oxide as the isolation layer. Therefore, to prevent repetition, the process flow about BC-OTFTs with *isolation* structure can refer to that section. Contrarily, a *conventional* BC-OTFT structure is shown in Fig. 6-12, where no field oxide layer under the S/D electrodes. This would cause a significant gate leakage through the large common gate electrode, collected by the S/D electrodes, and misleads the extraction of many electrical parameters of OTFTs. We will compare these two structures in the following section.

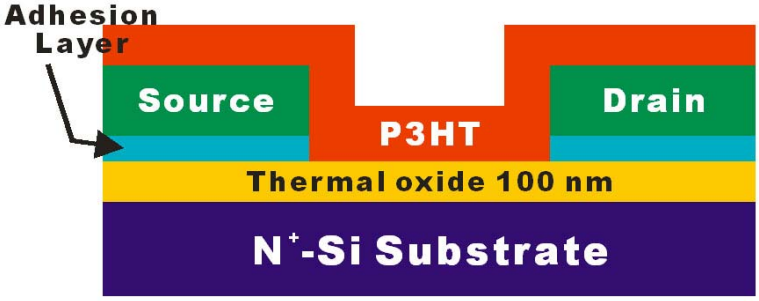

Figure 6-12 Schematic diagram of a conventional BC-OTFT

6.4.2 Results and Discussion

Figure 6-13 shows the typical output characteristics and transfer curves of a TC-OTFT. The electrical characteristics of OTFTs are similar to a conventional MOS, for output current increasing linearly at low drain bias and then saturating (channel pinch-off) at a high drain bias. Notably, the field-effect mobility for a top contact OTFT reaches 10^{-2} cm^2/Vs while the μ_{FE} of a BC-OTFT is only 7×10^{-4} cm^2/Vs. It is speculated that the P3HT forms a better crystallinity on a flat surface than that on the metal or its sidewall. Furthermore, for top-contact configuration, the external electric field induced by V_{GS} bias modifies the current conduction properties of the OTFT regions under contacts so that the contact resistance is lowered [6.46]. Both of these phenomenons could increase the extracted value of effective mobility. Although TC-OTFTs generally have higher mobility, the source/drain electrodes must be patterned through a shadow mask rather than photo-lithography (since solvents of P.R. and the developer would damage the organic active layer) and therefore the dimension cannot be precisely controlled. Consequently, we utilized BC-OTFT configuration throughout these experiments.

The electrical characteristics of OTFTs without the thick field oxide layer as shown in Fig. 6-12 were plotted in Fig. 6-14(a) and Fig. 6-14(b). Figure 6-14(a) compares the source current I_S and the gate leakage current I_G with the gate voltage V_G, while Fig. 6-14(b) illustrates the I_S - V_D curves of the OTFTs. The gate leakage current increases rapidly, becoming comparable to I_S as the magnitude of V_G increases. This anomalous leakage current not only deteriorates the electrical characteristics of transfer curves but also causes the overestimation of the device mobility. Moreover, the gate leakage is also responsible for the curve splitting phenomenon in Fig. 6-14(b) at $V_D = 0$ V, making OTFT consume power continuously without an external drain bias.

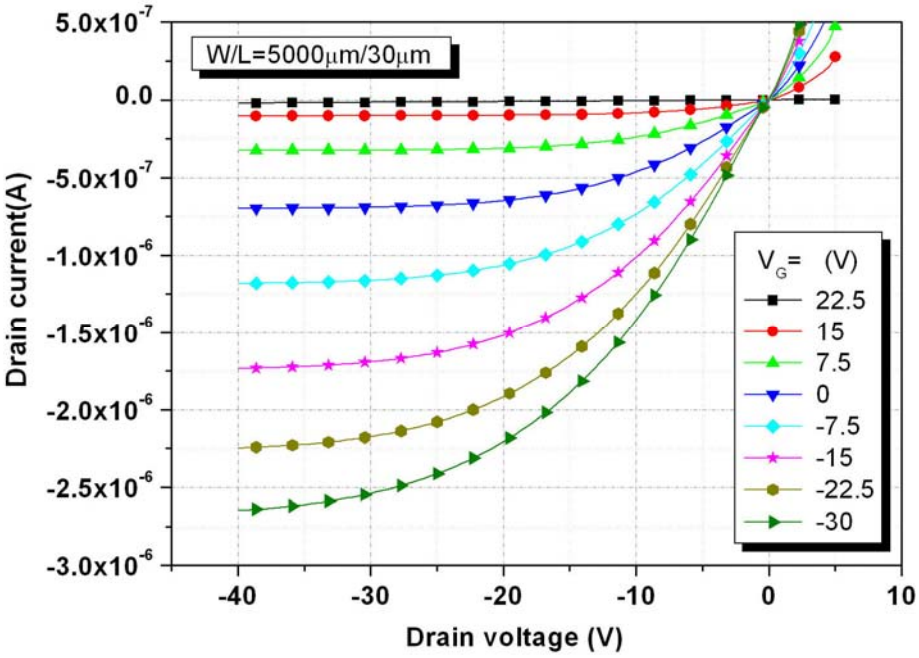

(a)

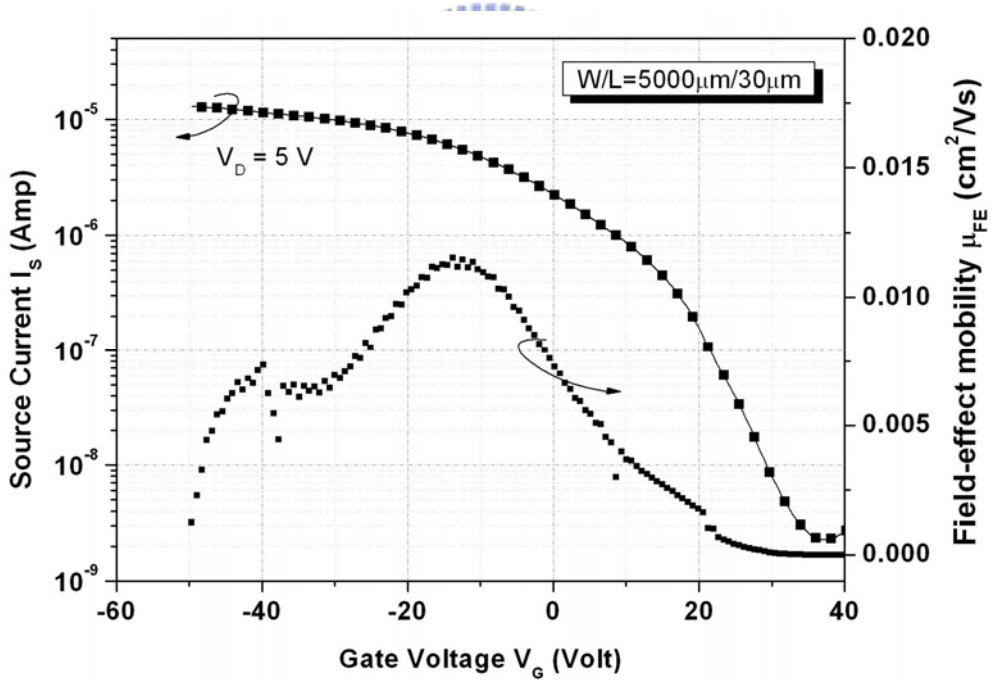

(b)

Figure 6-13 (a) I_D - V_D and (b) I_D - V_G curves of a TC-OTFT

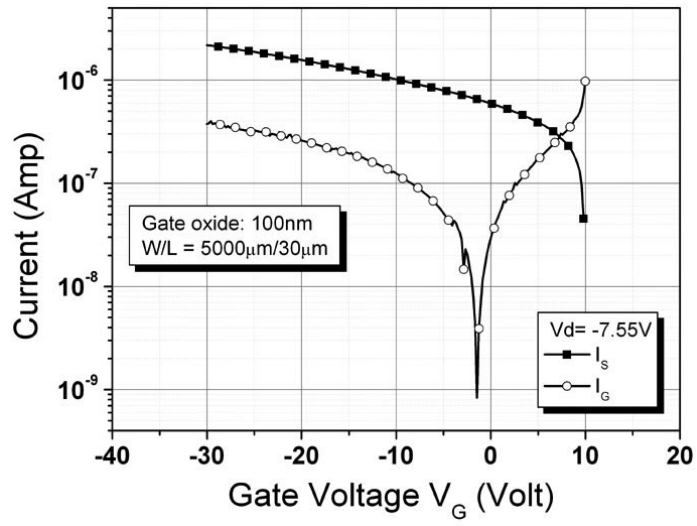

(a)

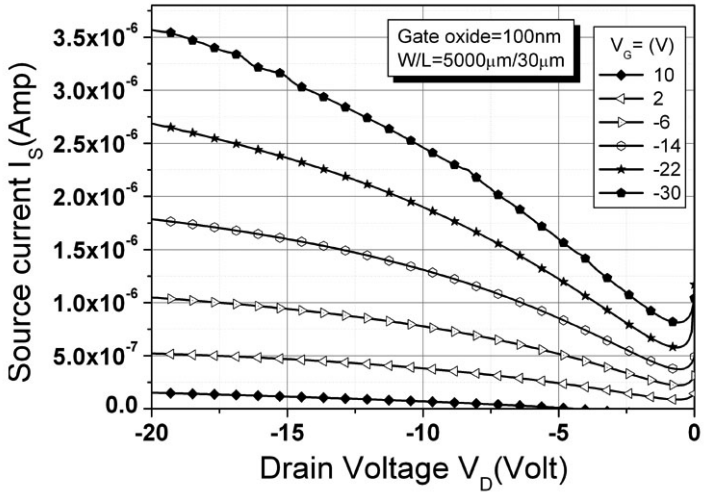

(b)

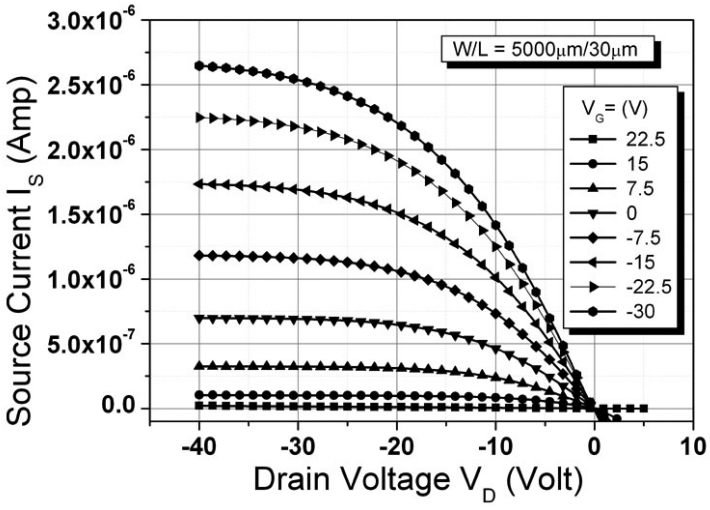

(c)

Figure 6-14 (a) I_S (I_G) - V_G and (b) I_S - V_D curves of the OTFTs without the field oxide layer, (c) I_S - V_D curves of the OTFTs with field oxide layer to eliminate the gate leakage current

To clarify the origin of the leakage current, MOS capacitors as shown in the embedded part of Fig. 6-15 were fabricated and then spun on chloroform or P3HT (0.3% wt. in chloroform), respectively. Figure 6-15 plots the gate leakage current density (extracted at 2 MV/cm) of the MOS capacitors treated in various ways. Although the capacitor having been treated with chloroform exhibits almost the same electrical characteristics as the untreated capacitor, the leakage current density of MOS-C with P3HT is at least three orders of magnitude higher. The leakage current did not increase with the organic contamination such as chloroform. For MOS-C with P3HT treatment, it is also noticeable that the leakage current density distributes widely from 10^{-5} to 10^{-3} A/cm^2, and the leakage current density at V_g = + 40 V is two orders of magnitude larger than that at V_g = - 40V. Accordingly, the additional leakage paths were assumed to be associated with the conductive P3HT film rather than the actual area of the top plate (Pt). Specifically, the conductive P3HT film connected the additional leakage paths of the insulator, increasing the effective area of the capacitor's top plate and, therefore, the leakage current; when a large negative gate bias was applied, the P3HT film became depleted and less conductive, contributing to a smaller effective area of the capacitor's top plate.

Two methods are available for alleviating the anomalous gate leakage in an OTFT. One is to pattern the active area, for which the P3HT can be dropped onto a specific place by micro-printing technology, or can be etched away using UV light or O_2 plasma [6.21], [6.47], [6.50]. The second method, utilized in this work, is to form a thick field oxide layer on the wafer surface except in the gate region. The leakage current density of the field oxide is lower than that of the thin gate oxide; moreover, the P3HT film upon the field oxide does not accumulate and becomes less conductive as the (bottom) gate bias decreases. To reduce the process temperature, the field oxide layer can be fabricated by ECR-PECVD or liquid-phase deposition system at room temperature without sacrificing the function of isolating structure [6.48], [6.49]. As shown in Fig. 6-14(c), the field oxide layer successfully eliminated the

leakage current from the gate to the source/drain electrodes, so no curve splitting phenomenon was observed at the origin of I_S - V_D curves.

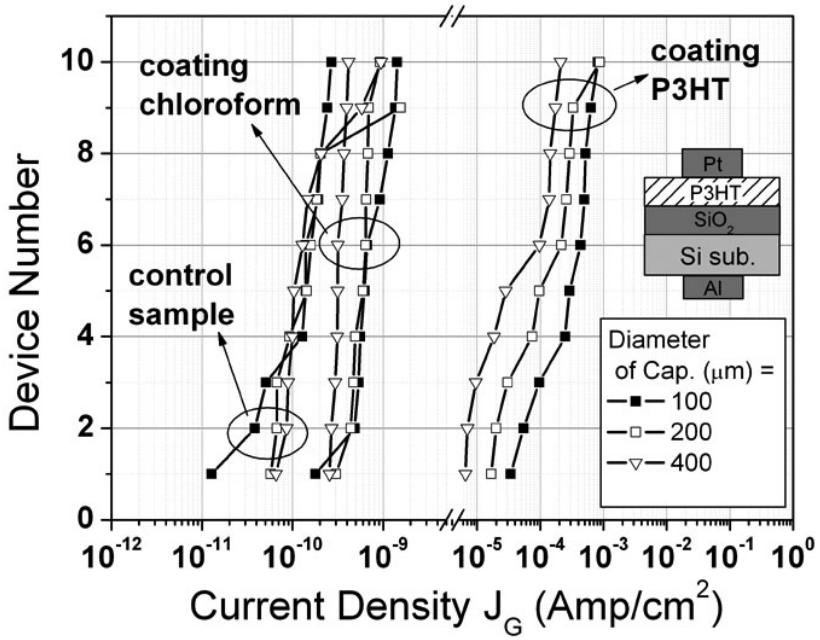

Figure 6-15 Comparison of gate leakage current density for MOS capacitors with different organic treatments.

6.5 Source/Drain Metals for Ohmic Contact with P3HT

Despite the considerable progress made in recent years in improving the performance of organic TFTs, many of the design, material, and process parameters impacting organic TFT performance are still poorly understood and poorly controlled. One such parameter is contact resistance. Unlike the field-effect transistors based on inorganic silicon material, the source/drain contacts in organic TFTs cannot be easily optimized by conventional processes such as doping or silicidation [6.50]. Thus except low mobility, OTFTs performance also suffers from large contact resistance.

Various attempts have been made to modify the surface potential energy of S/D metals, enhancing the charge injection efficiency from S/D to the organic active layer. These methods

include surface treatment by self-assembling molecular monolayer with hexamethyldisilane (HMDS) or octadecyltrichlorosilane (OTS), and pretreatment by O_2 plasma for a short time [6.51]-[6.54]. On the other hand, the metal work function has great influence for determining a metal/P3HT interface to be ohmic or not. The source/drain material typically used in P3HT based OTFTs is Au or Pt. However, these noble metals are quite expensive so we hope to find out the other metals to replace them. In this section, different contact metals would be examined and the influence of the adhesion layer thickness is also clarified.

6.5.1 Experimental

The BC-OTFT structure with field isolation was utilized in this experiment. The related process can refer to Section 6.3.1 and will not be repeated here.

After the photo-lithography process of S/D definition, four kinds of electrode materials including Ti, Ni, Pt and Au were evaporated by Dual E-Gun evaporation system with a thickness of 100nm and then the source/drain electrodes were patterned by lift-off method. For Ni, Pt and Au, an additional 20nm thick Ti must be used as an adhesion layer. Moreover, we also adjusted the thickness ratio of adhesion/contact metals: Ti/Pt =20nm/100nm, Ti/Pt = 100nm/20nm, Ti/Au = 20nm/100nm and Ti/Au = 100nm/20nm. Finally, P3HT film was spin coated on the samples to complete the OTFTs.

6.5.2 Relationship of S/D Metals and the Performance of OTFTs

Figure 6-16 shows the variation of threshold voltage and linear mobility as a function of the channel length. As expected, the field-effect mobility gradually increases with the channel length, since for a shorter channel length, the contact resistance is dominate.

For a constant W/L ratio, the effect of contact resistance can be clearly observed in the output characteristics of OTFTs with different channel length. Figure 6-17 exhibits the output drain current at two gate voltages (-20 V and -25 V) for devices with channel length of 50, 25

and 15 μm. At a drain voltage of -30 V, a 50% reduction in drain current is observed as the channel length decreased from 50 to 25 μm. The drain current saturates at an increasingly higher drain voltage when the channel reduced to 15 μm. These observations can be attributed to the lower field-effect mobility, a larger threshold voltage, or both, because of the increased percentage of the contact resistance to the total channel resistance.

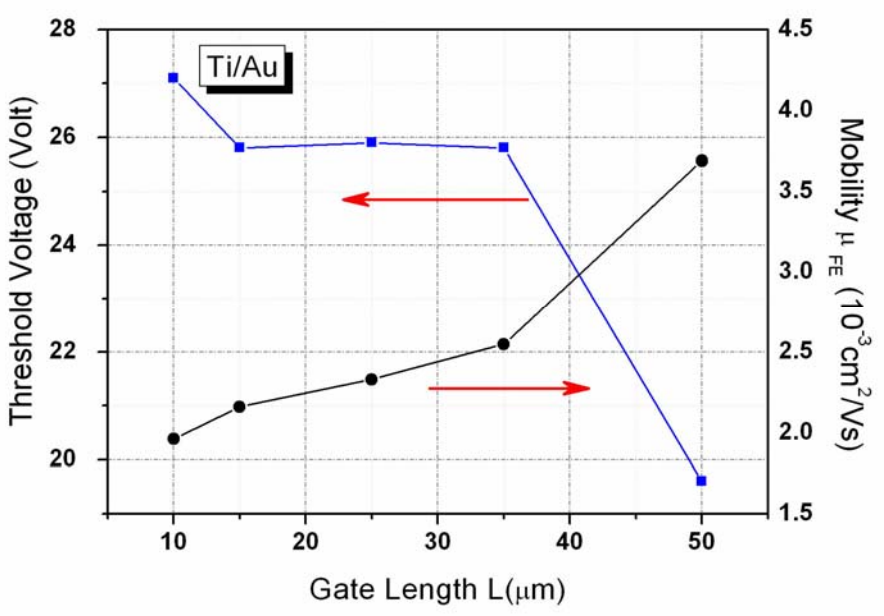

Figure 6-16 The variation of threshold voltage and linear mobility as a function of the channel length

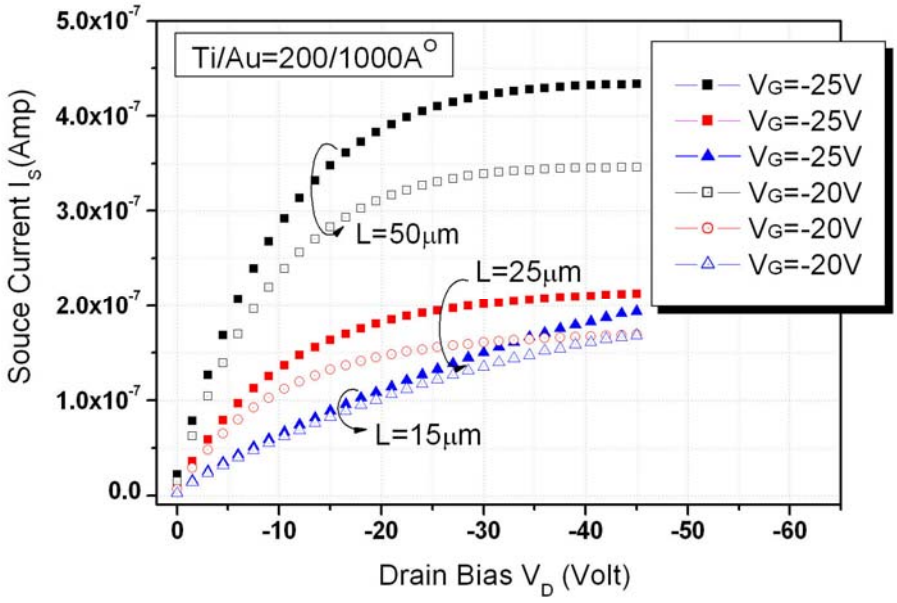

Figure 6-17 Output characteristics of OTFTs with different channel length of 50, 25, and 15 μm; the W/L ratio = 20

As a p-type semiconductor, P3HT can form an ohmic contact with metal for work function larger than 4.5 eV. Therefore, for Ni (φ_F = 4.84 eV), Pt (φ_F = 5.29 eV) and Au (φ_F = 4.58 eV) is supposed to be contact metals with P3HT. In contrast, because work function of Ti (φ_F = 4.09 eV) is smaller than 4.5eV, Ti forms a Schottky barrier with P3HT; it cannot be observed a normal output characteristics, as shown in Fig. 6-18.

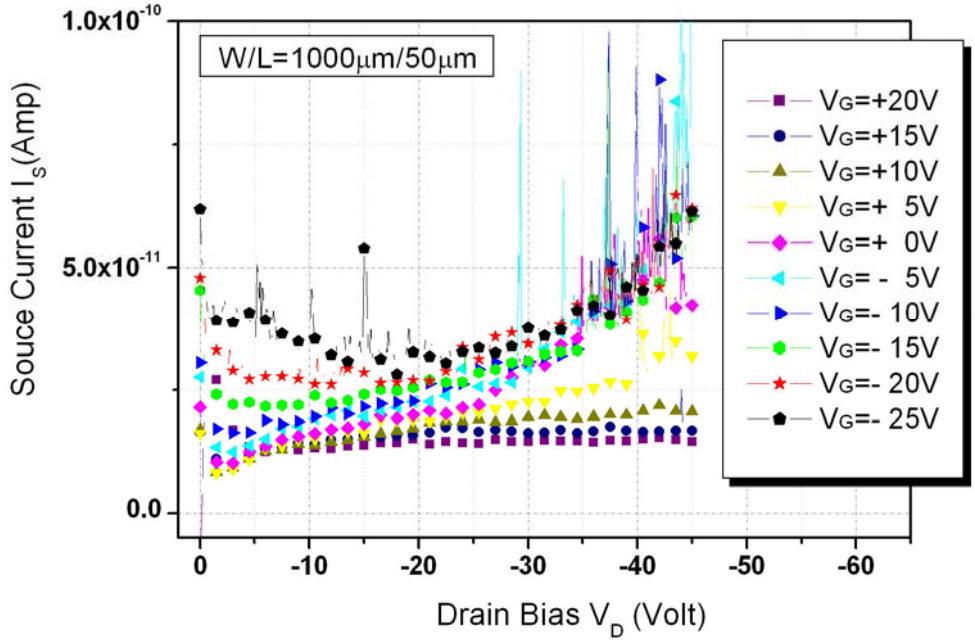

Figure 6-18 Output characteristics of OTFTs with Ti as the S/D electrodes

Figure 6-19(a) and (b) illustrate the I_S - V_D curves of OTFTs with Ti/Ni and Ti/Pt as the S/D electrodes, respectively. From Fig. 6-19(a), it can be found that the crowding effect occurs at a small drain bias near zero voltage while the OTFTs with Pt S/D exhibits satisfactory linear characteristics as shown in Fig. 6-19(b). Such larger contact resistance is attributed to the work function mismatch between Ni/P3HT and potential chemical reactions of Ni with sulfur atoms in P3HT, forming an interfacial layer at the Ni/P3HT interface [6.55], [6.59]. The crowding effect can be successfully eliminated by depositing another thin Pt layer above the Ni metal, as shown in Fig. 6-19(c).

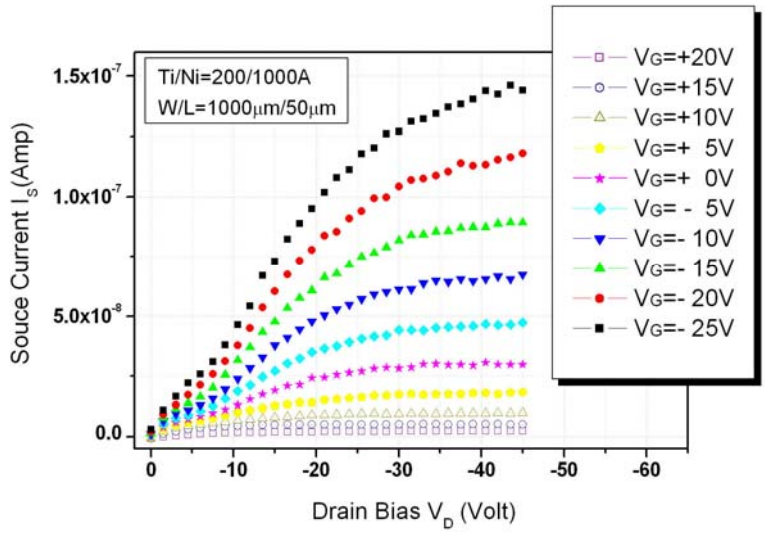

(a)

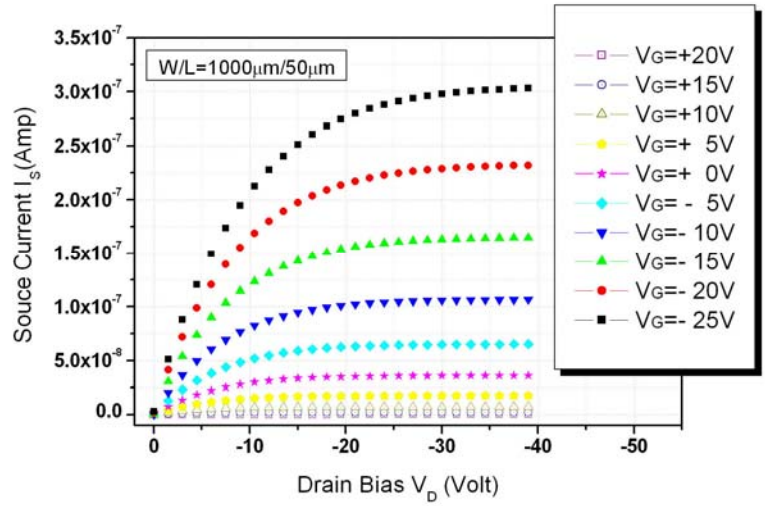

(b)

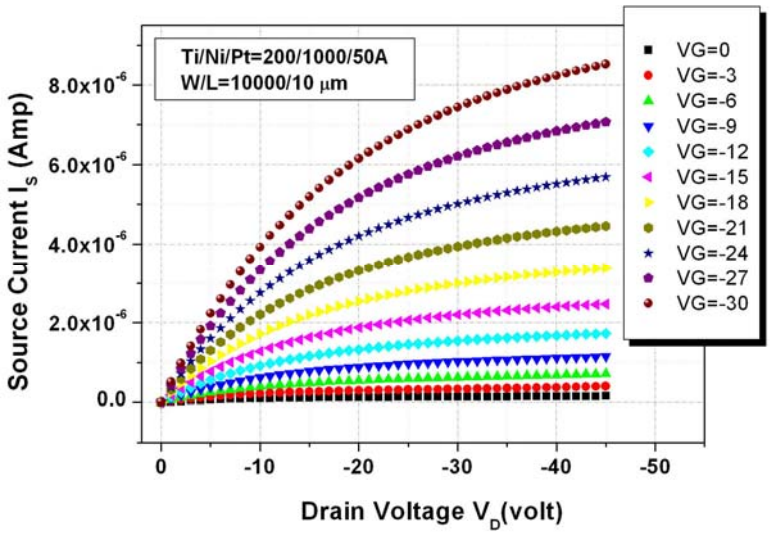

(c)

Figure 6-19 Output characteristics of OTFTs with (a) Ti/Ni, (b) Ti/Pt, and (c) Ti/Ni/Pt as the S/D electrodes

6.5.3 Effect of Adhesion/Contact Material ratios to the Contact Resistance

The total contact and series resistance can be estimated by plotting the inverse of drain current versus channel length, extrapolating to a channel length of zero (where the channel resistance disappears), and multiplying by the drain-source voltage. For each device with L ranging from 10 to 50 μm, the drain current was measured at -1V and -5V for a gate voltage ranging from -5V to -30V. The resulting width-normalized ON resistance R_{on} W versus L is calculated and the contact resistance is a set of straight lines intersecting at a triangle area. The results are shown in Table 6-3. It shows that the contact resistance is not dependent on the composition of adhesion/contact materials at V_{DS} = -5 V; however, the contact resistance is dependent on the adhesion/contact thickness ratio at V_{DS} = -1 V and the contact resistance reduces as the adhesion/contact thickness ratio becomes smaller. Generally, ideal non-rectifying contacts would exhibit no resistance to the flow of current in either direction through the contact, and their I-V characteristics would appear as shown in Fig. 6-20(a). In practical, however, when the metal-to-semiconductor contacts are fabricated, they form a nonlinear ohmic contact as depicted in Fig. 6-20(b) owing to the charge trapping/de-trapping and the ion motion in the metal/P3HT interface [6.59], [6.60]. So it was observed that the contact resistance at V_{DS}= -1 V is larger than that at V_{DS} = -5 V.

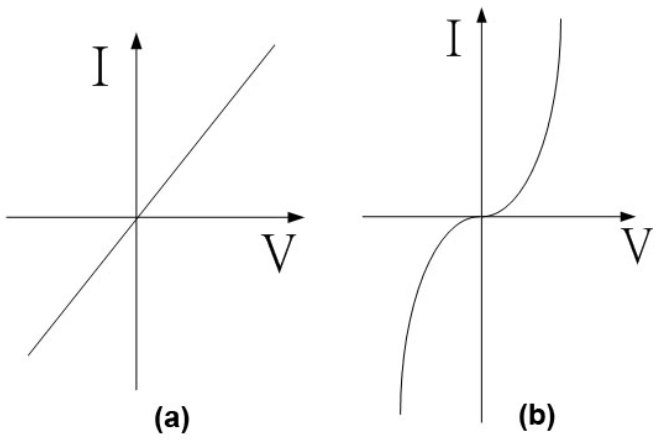

Figure 6-20 I-V characteristics of contacts between metal and semiconductor in integrated circuits: (a) ideal ohmic contact and (b) nonlinear ohmic contact

Table 6-3 Contact resistance between S/D electrodes and P3HT

Source/Drain Metals	Contact Resistance ($\times 10^6$ Ω-cm)	
	V_{DS} = -5 V	V_{DS} = -1 V
Ti/Pt = 200Å/1000Å	0.3	1.0 ~ 2.5
Ti/Au = 200Å/1000Å	0.25	0.4 ~ 0.5
Ti/Pt = 1000Å/200Å	0.3 ~ 0.4	4.5 ~ 6.0
Ti/Au = 1000Å/200Å	0.3 ~ 0.35	1.0

The slope of $R_{on}W$ versus L, i.e., the channel sheet conductance, contains only intrinsic device parameters independent of the channel length. Therefore, by plotting the reciprocal of the slope, $[R_{on}W/\Delta L]^{-1}$ versus gate voltage V_G, as given in Fig 6-21, the slope of linear least-square curve fit provides the field-effect mobility in the linear regime. The extracted μ_{FE} with Ti/Pt as contact metal is 2.22 $\times$ 10^{-3} cm^2/Vs. This value is quite close to the mobility (2.1 $\times$ 10^{-3} cm^2/Vs) measured for a OTFT with long channel.

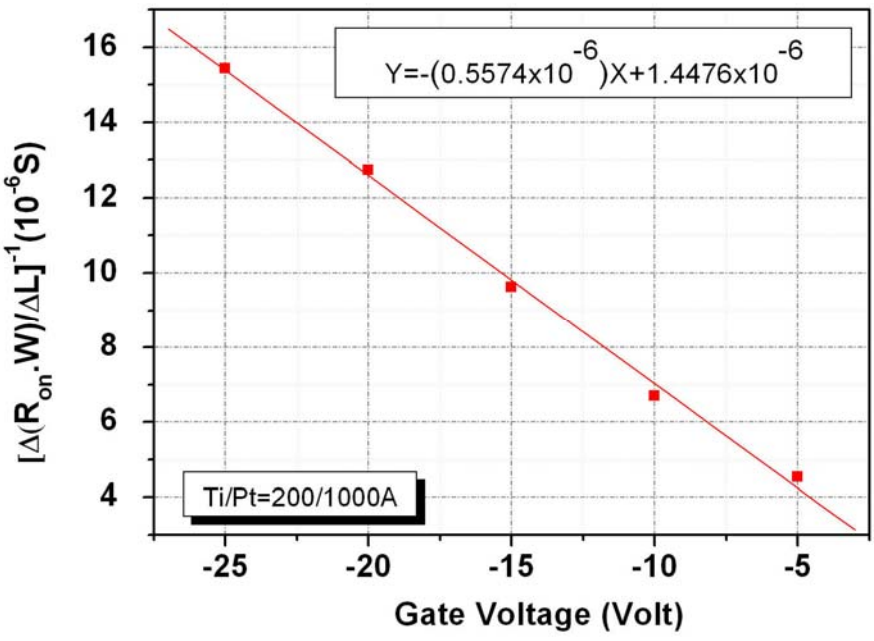

Figure 6-21 OTFT channel sheet conductance as a function of gate voltage; S/D metal is Ti/Pt

Finally, the effect of the adhesion layer can be clearly observed by varying the thickness of Ti to 2 ~ 100 nm and keeping the thickness of Pt in 100 nm. The averaged ON current of OTFTs with different adhesion layer/contact metal ratios were depicted in Fig. 6-22. Since the Ti forms Schottky barriers with P3HT and hinders the carrier injection rate, the ON current decreases with increasing the thickness of titanium. Consequently, in order to keep a reasonable thickness of the source/drain metal while decrease the Ti layer as thin as possible, a stacking structure like Ti/Ni/Pt was recommended.

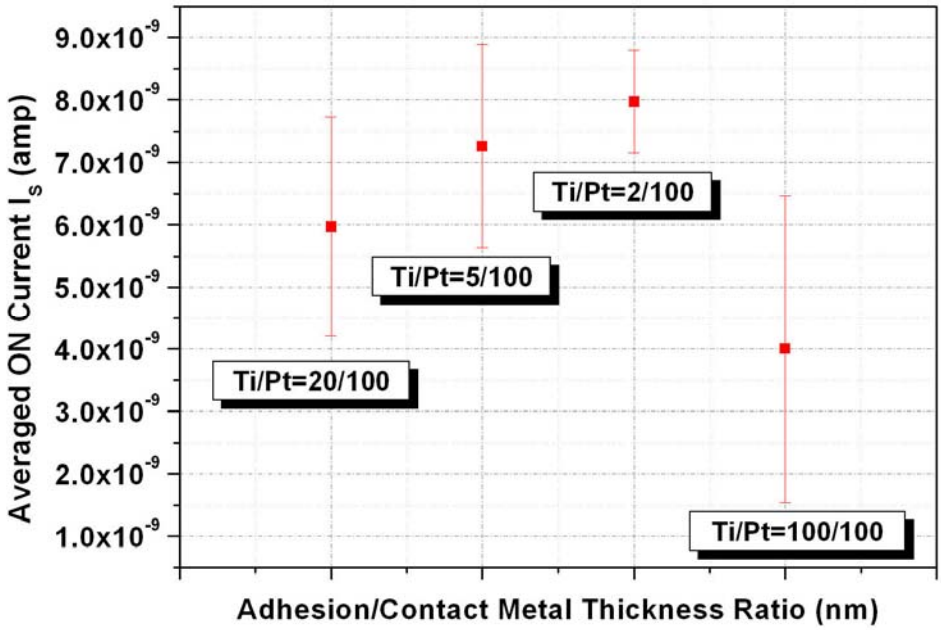

Figure 6-22 Averaged ON current versus different adhesion layer/contact metal ratios

6.6 Summary

In this section, we examined the physical properties of P3HT deposited with different solvents and weight percentages through AFM and SEM measurements. The P3HT film fabricated with a wt. % of 0.3 in chloroform was found to exhibit the lowest surface roughness and high ON/OFF current ratio and carrier mobility. Besides, the reason for the anomalous gate leakage current was clarified, and this current was eliminated by the thick

field oxide layer on S/D regions.

For contact resistance measurements, we proved that metals with work function higher than P3HT such as Ni, Pt, Au, etc. would form an ohmic contact. In addition, a Pt cap layer can be added to prevent the growth of interfacial layer in the Ni/P3HT interface and thus eliminate the crowding phenomenon at the output characteristics of OTFTs. It also suggested that the production cost of OTFTs can be reduced by replacing a thick Pt electrode with a combination of thick Ni and a thin Pt capping layer.